

Effect of boundary conditions on axial flow in a concentrated vortex core

Richard K. Cohn and Manoochehr M. Koochesfahani

Department of Mechanical Engineering, Michigan State University, East Lansing, Michigan 48824

(Received 28 May 1992; accepted 17 August 1992)

The character of axial flow in the core of a concentrated line vortex is studied using flow visualization. Results show that axial flow can be initiated when the no-slip boundary condition is imposed on the vortex core over a spatial extent comparable to the core diameter. It is further demonstrated that no-slip is not a necessary condition to generate the axial flow; a region of spanwise shear (i.e., a slip boundary) is sufficient. Two distinct axial flow velocity profiles are observed; they are either jetlike or spatially undulated corresponding to a maximum axial speed occurring at the core center or outer edge, respectively.

An important feature of most concentrated vortices is the existence of axial flow in their cores. Some notable examples are wing-tip vortices, vortex breakdown over delta wings, geophysical vortices (e.g., tornadoes), and a number of confined flows such as vortex chambers, and swirl separators (e.g., hydrocyclones). More recently, Koochesfahani¹ has reported observations of axial flow in the vortices shed from the trailing edge of a rapidly oscillating two-dimensional (2-D) airfoil. The axial motion takes the form of a spiraling of the vortex core fluid away from the side walls of the flow facility toward the centerline. Similar observations have also been reported by Kurosaka *et al.*² in a forced two-stream shear layer and in the von Kármán vortex street behind a circular cylinder. In both studies,^{1,2} axial flow was argued to be the result of the no-slip boundary condition enforced by the side walls on the shed vortices. By the nature of the experimental arrangement in these two investigations, the no-slip boundary condition was imposed on the vortex tubes at all times as the vortices convected downstream.

The present experimental study addresses two specific issues. The first is the spatial extent (i.e., minimum distance) over which the no-slip boundary condition needs to be enforced on a vortex core in order to initiate axial motion. We note the utility of this information to the design of intrusive probe measurement techniques in such flows. The second issue is whether the no-slip boundary condition is necessary at all for the axial flow to begin.

The experiments were performed in a water channel (Engineering Laboratory Design, Inc.) with a free-stream speed of $U_\infty = 15$ cm/sec. Concentrated line vortices were generated by an NACA 0012 airfoil pitching sinusoidally ($f = 4$ Hz) about the quarter-chord axis around a zero mean angle of attack with an amplitude of about 2° . The airfoil had a uniform chord of $C = 8$ cm, a span of $b = 45$ cm, and was fitted on both ends with false walls parallel to the water channel walls. See Koochesfahani¹ for details of the setup and the resulting vortical flow field. Detailed analysis of this flow field at the midspan location at $x/C = 1$ (where 3-D effects are negligible) indicates that the vortex field is well represented by an array of Gaussian core vortices whose core radius R_0 and circulation Γ_0 are approximately 0.24 cm and 22.8 cm²/sec, respectively.³ The vortex Reynolds number, $Re_v = \Gamma_0/\nu$, is therefore about 2280;

the aspect ratio of the vortices, defined by the ratio of vortex length to core diameter, is approximately 94. Throughout this paper, we will use the vortex core radius R_0 as the reference length scale.

The flow field within the shed vortices was visualized using laser-induced fluorescence (LIF). A fluorescent dye (fluorescein) originated from five injection tubes imbedded in the trailing edge of the airfoil at equidistant spanwise locations approximately one chord length apart, as shown in Fig. 1. The dye labeled the formation of the vortical region in a jelly roll pattern. As the vortex convected downstream, an axial dye displacement indicated the axial flow within the core. The dye displacement field, at a given downstream location, was monitored by an argon ion laser sheet placed parallel to the vortex axis and normal to the free-stream flow direction, i.e., in the (y - z) plane (see Fig. 1). The fluorescence intensity, viewed through the downstream window of the flow facility (i.e., along x direction), was recorded by an electronically shuttered CCD camera on standard videotape. The images were subsequently digitized and enhanced using a digital image processor (Recognition Concepts Inc., Trapix-5500) to produce outlines of the dye displacement boundary. The images of the dye displacement field selected for discussion here were chosen to be representative of the character of the axial flow as the vortex center (as opposed to its edges) passes through the laser sheet. Note that the dye displacement field at station x is indicative of the integrated axial velocity field from the airfoil trailing edge, and not the instantaneous velocity field.

Results are first presented for the case where the no-slip boundary condition is enforced only by the false side walls. Figure 2 shows the displacement field of dye originating from injectors 1–3. The spanwise coordinates of these injectors (i.e., origin of dye) are $z/R_0 = 31.25, 62.50,$ and 93.75 , respectively. A jetlike axial flow, with maximum flow speed at the core center, can be seen which transports fluid from the side walls toward the channel centerline. Dye injector 3, which is located at midspan, does not register any axial flow.

To impose the no-slip boundary condition on the vortex core over a finite spatial extent, various symmetrical two-dimensional objects were placed near the trailing edge of the airfoil between dye injectors 2 and 3 (see Fig. 3).

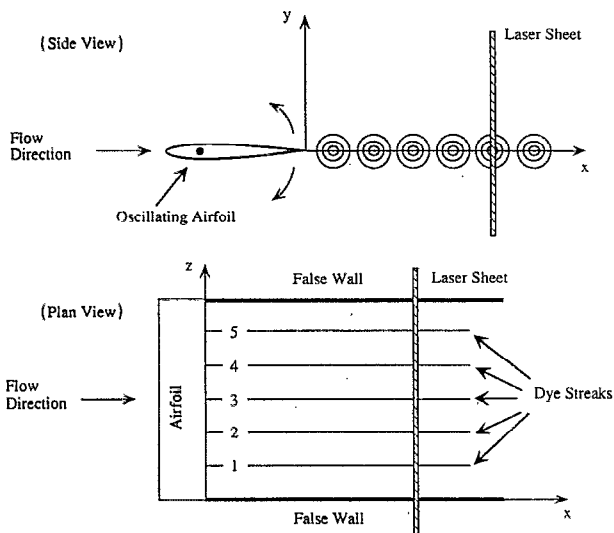


FIG. 1. Schematic of LIF visualization arrangement.

These objects were positioned in the $(x-y)$ plane with their long axes parallel to the y coordinate. Both airfoil-shaped streamlined bodies and flat plates with streamlined leading/trailing edges were utilized as boundary objects. The streamwise extent L of the boundary objects varied in the range $2.6 \leq L/R_0 \leq 380$ in vortex core units. Their thickness t was in the range $1.3 \leq t/R_0 \leq 2.6$.

The dye displacement field at $x/R_0 = 43$ for two no-slip boundary objects of length $L/R_0 = 32$ and 4 is shown in Fig. 4. Note that axial flow indicated by injectors 2 and 3 is now in a direction away from the finite-length no-slip boundary object, and is jetlike. Dye injector 1 shows axial flow away from the false wall as discussed before. The most striking result is that a boundary object length as small as $4R_0$ is sufficient to induce axial flow, and the resulting flow is comparable to that induced by the longer object of length $32R_0$. Similar axial flow pattern was observed for the entire range of boundary object lengths L/R_0 tested here. This pattern was also similar to that reported in Ref. 1 for the case $L/R_0 \rightarrow \infty$. It was noted, however, that using

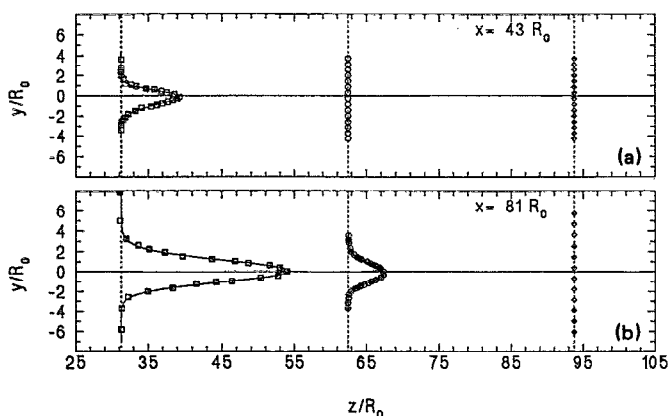


FIG. 2. Dye displacement field due to no-slip condition at the false wall at two different downstream locations.

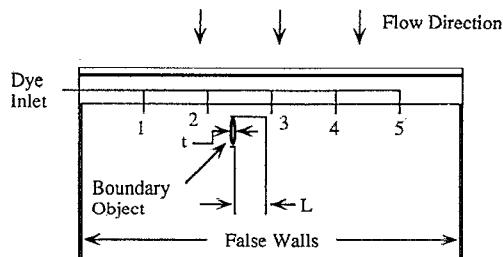


FIG. 3. Schematic of finite-length boundary object placement.

a very thin wire of diameter $(0.02R_0)$ as a boundary object did not lead to any observable axial flow. We were unable to determine a minimum length over which the no-slip boundary condition must be imposed in order to initiate axial flow. The results presented show, nevertheless, that no-slip over a spatial extent of the order of core diameter is certainly sufficient to induce axial flow. We draw attention to the implications of these findings to the usage of intrusive probes to study such vortex flows; the probe must be significantly smaller than the core diameter, otherwise its mere presence will alter the flow character.

In order to examine whether the no-slip boundary condition is necessary for the onset of axial flow, the various boundary objects used earlier were placed upstream of the airfoil as indicated in Fig. 5. The wake region thus created may be thought of as enforcing a slip (or shear) boundary condition on the vortices as they form downstream of the airfoil. The dye displacement field at $x/R_0 = 43$ for two spanwise placement of the wake boundary is shown in Figs. 6(a) and 6(b). The presence of axial flow is once again marked by injectors 2 and 3, suggesting that no slip is not a necessary boundary condition to initiate axial flow.

The intriguing result in Figs. 6(a) and 6(b) is that two fundamentally different types of axial flow profiles are now observed. The dye injector farther away from the wake boundary exhibits the jetlike profile, while the one closer to the wake boundary displays a spatially undulated profile corresponding to an axial flow where the maximum speed

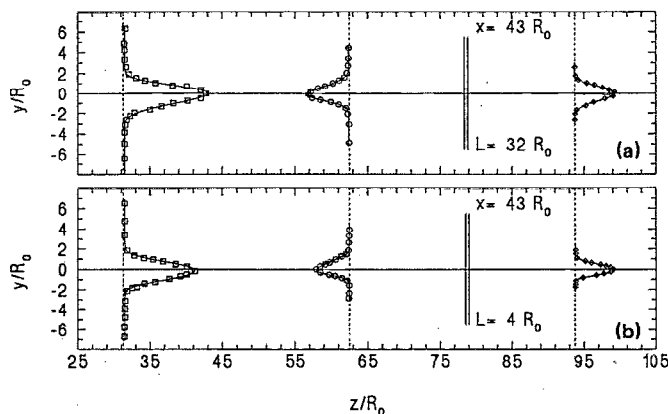


FIG. 4. Dye displacement field for finite-length no-slip boundary objects. The spanwise location of the object is indicated by the two parallel vertical lines.

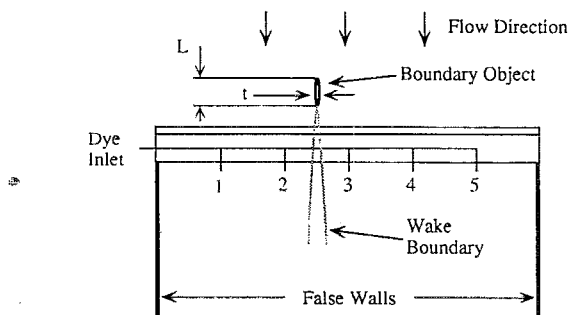


FIG. 5. Schematic of wake generating body placement.

occurs at the outer edge of the vortex core with very little motion at the core center. Note that dye injector 1 still shows the jetlike behavior due to the no-slip boundary condition imposed by the false wall. It is interesting to observe the large spanwise variation of the axial velocity profile within the vortex tube. These features persist at $x/R_0=81$, as illustrated in Fig. 6(c) for the case of a wake-generating object placed nearly equidistant between injectors 2 and 3. Dye injector 3 once again shows a displacement field indicative of an axial flow with zero speed at the center and maximum speed at the outer core. The appearance of a reverse flow region at the vortex center indicated by injector 2 should be treated with caution in the absence of instantaneous velocity measurements. Note that, at this x station, injector 2 already exhibits axial flow at the core

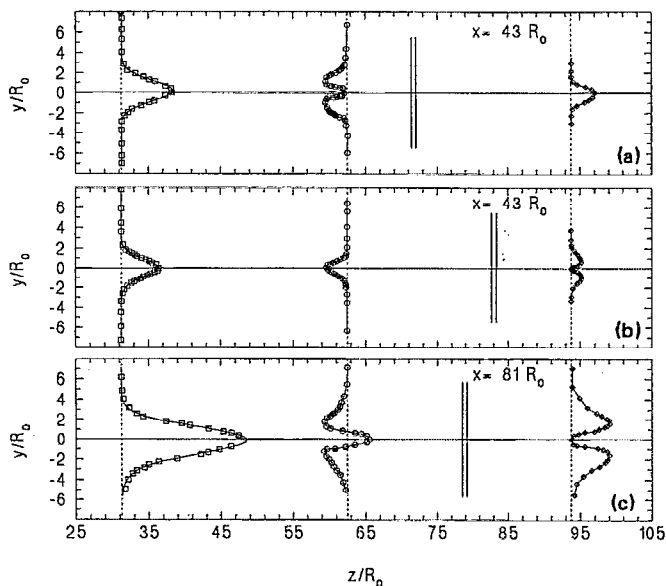


FIG. 6. Dye displacement field for wake boundary. The approximate spanwise location of the wake-generating object is indicated by the parallel lines.

center because of the no-slip boundary condition of the false wall [see Fig. 2(b)].

The various axial velocity profiles we have observed are similar to some of the similarity solutions of Donaldson and Sullivan,⁴ which were derived with confined vortices in mind. Their solutions assumed an axial profile invariant along the vortex span; this assumption does not apply in the flows reported here. We also mention that the 3-D velocity field inside a realistic vortex exposed to the simplest boundary condition of no slip does not seem to have been solved. By a realistic vortex, we mean one that has a finite core of, say, Gaussian vorticity distribution, and an outer irrotational flow. The difficulties in obtaining a solution for this flow are described by Kuo,⁵ who instead provides an approximate solution using a momentum integral approach. Clearly, further experimental and analytical work are needed in this area. We would mention that vortex axial flows can provide a very strong transport mechanism; speeds along the core comparable to the maximum swirl speed have been noted in our experiments. The spanwise transport documented recently by Kotidis⁶ behind the rotor blades of a compressor stage, which is believed to be responsible for the drop in the tip efficiency, is also possibly a manifestation of phenomena similar to those reported here. We further note that, according to one of our reviewers, the fact that no slip is not necessary for the axial flow has also been demonstrated by Torres⁷ in a study of a cylinder placed behind a V-shaped shear.

ACKNOWLEDGMENTS

We acknowledge T. Brown, C. MacKinnon, and S. Chakrabarti for their help with this research. We are particularly grateful to Dr. M. Khorrami for helping us with some of the references.

This work was supported by MSU's Honors College, College of Engineering Summer Research Internship Program, Division of Engineering Research, and the Air Force Office of Scientific Research Grants No. AFOSR-89-0417 and No. AFOSR-89-0130.

¹M. M. Koochesfahani, "Vortical patterns in the wake of an oscillating airfoil," *AIAA J.* **27**, 1200 (1989).

²M. Kurosaka, W. H. Christiansen, J. R. Goodman, L. Tirres, and R. A. Wohlman, "Crossflow transport induced by vortices," *AIAA J.* **26**, 1403 (1988).

³M. M. Koochesfahani and J. M. Stempky, "Velocity and vorticity fields in the wake of a rapidly pitching airfoil," *Bull. Am. Phys. Soc.* **34**, 2306 (1989).

⁴C. Du P. Donaldson and R. D. Sullivan, "Examination of the solutions of the Navier-Stokes equations for a class of three-dimensional vortices. Part I. Velocity distributions for steady motion," *Aeronautical Research Associates of Princeton*, Report No. AFOSR TN60-1227 (1960).

⁵H. L. Kuo, "Axisymmetric flows in the boundary layer of a maintained vortex," *J. Atmos. Sci.* **28**, 20 (1971).

⁶P. A. Kotidis, "Unsteady radial transport in a transonic compressor stage," Ph.D. thesis, Massachusetts Institute of Technology, GTL Report No. 199 (1989).

⁷L. Torres, M.S. thesis, University of Tennessee Space Institute, 1988.